Controllable thermal expansion of large magnitude in chiral negative Poisson's ratio lattices

Chan Soo Ha, Eric Hestekin, Jianheng (Harry) Li, Michael E. Plesha, Roderic S. Lakes*

July 28, 2015

Department of Engineering Physics, University of Wisconsin, Madison, WI 53706-1687, USA
Keywords (chirality, negative Poisson's ratio, auxetic, thermal expansion)
∗ Corresponding author. email lakes@engr.wisc.edu Phone: +00 608 265 8697
Preprint of Ha, C. S., Hestekin, E. , Li, J., Plesha, M. E., Lakes, R. S., "Controllable thermal expansion of large magnitude in chiral negative Poisson's ratio lattices", Physica Status Solidi B, 252(7), 1431-1434 (2015).

Abstract

Lattices of controlled thermal expansion are presented based on planar chiral lattice structure with Poisson's ratio approaching -1. Thermal expansion values can be arbitrarily large positive or negative. A lattice was fabricated from bimetallic strips and the properties analyzed and studied experimentally. The effective thermal expansion coefficient of the lattice is about $\alpha = -3.5 \times 10^{-4} \mathrm{K}^{-1}$. This is much larger in magnitude than that of constituent metals. Nodes were observed to rotate as temperature was changed corresponding to a Cosserat thermoelastic solid.

1 Introduction

Materials with large thermal expansions have many potential applications as thermal actuators. Available materials such as common metals, alloys, and polymers have a limited range of expansion that may not suffice for some applications. Composite materials may be considered, but until recently were not thought to be promising, because thermal expansion of a two phase composite has been constrained by analytical bounds [1]. The expansion of the composite cannot be larger than the maximum expansion of the constituents. These bounds were derived assuming that the two phases are perfectly bonded, also that there is no porosity, and that each phase has a positive definite strain energy. If one relaxes any of these assumptions, one can achieve arbitrarily large or small values of expansion. For example if the composite contains void space, lattices may be envisaged with controllable expansion of large or small magnitude, or even negative expansion [2] [3]. The ribs in the lattice can be made of a sandwich of two materials of different thermal expansion, giving rise to bending [4]. In a related vein, lattices with bi-material piezoelectric elements have been developed and analyzed [5] and studied experimentally [6]; these lattices give rise to large values of piezoelectric sensitivity.

The concept used in the present research is based on a planar chiral lattice with Poisson's ratio -1 [7]. The Poisson's ratio was determined experimentally and analytically. Experiments revealed that the Poisson's ratio is approximately constant for axial compressive strains up to 25%. This is in contrast to the nonlinearity observed in the Poisson's ratio of negative Poisson's ratio foams [8] and of honeycombs [9] with inverted hexagonal cells of bow-tie shape. Negative Poisson's ratio

materials are commonly referred to as "auxetic". Chiral lattices have been analyzed [10] in the context of Cosserat (micropolar) elasticity [11] in which rotation of points has physical significance. Analysis shows this lattice has the largest Cosserat characteristic length scale of all known lattice topologies [12].

Chiral lattices have been considered for use as chiral honeycomb [13] [14] in sandwich panels for airplane wings that change shape, and they have been analyzed for buckling [15] and other characteristics such as stop bands in wave propagation [16]; they have also been fitted with sensors and actuators for possible use as smart structures [17].

2 Procedure

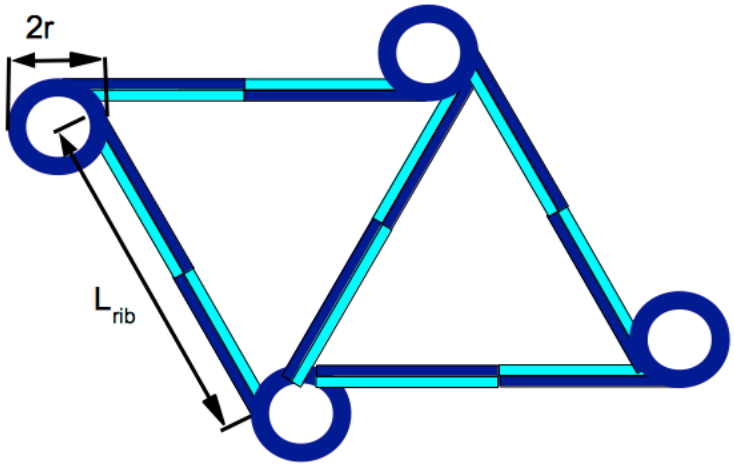

Figure 1: Chiral lattice structure with bi-material ribs with alternating orientation. Two materials indicated as light and dark, differ in their thermal expansion.

The lattice structure is chiral in plane and gives rise to a Poisson's ratio approaching -1. To achieve control of the thermal expansion, the lattice structure makes use of bi-material rib elements as shown in Figure 1. These ribs bend upon a temperature change, giving rise to node rotation and to strain of the lattice.

As for materials, the most active bimetallic strip material available was used: Engineered Materials Solutions "P675R" strip [18]. Its high expansion alloy is 52.8% by weight and is composed of 72% manganese, 18% copper, and 10% nickel. Its low expansion alloy is 36% nickel and 64% iron [18]. The thermal expansion coefficient for constituent metals is from about 10×10^{-6} K^{-1} (for iron) to 22×10^{-6} K^{-1} (for manganese). The low expansion alloy appears to be Invar, with $\alpha = 1.3 \times 10^{-6}$ K^{-1} and the high expansion alloy [19], $\alpha = 27.2 \times 10^{-6}$ K^{-1}.

The strips were first cut from a large roll of bimetallic sheet. The strips were cut to a length of $L_{rib} = 75$ mm, and a width of 10 ± 0.2 mm. The thickness of the strips is $h = 0.25 \pm 0.05$ mm. The high and low expansion sides were determined by heating a strip on a hot plate and observing the curvature. The circular nodes used for the chiral cells were cut from a chlorinated PVC plastic pipe with outer diameter $d = 16$ mm and wall thickness 2 mm. In an initial trial, a lattice was made by bonding constituents with conventional cyanoacrylate cement, but the glue joints did not survive repeated excursions to 70°C. Constituents were bonded with Loctite type 491 cement, intended for use at elevated temperature up to 400°C. The lattice cells were constructed following the design in

Figure 1 except that some overlap of rib segments was provided to facilitate bonding, rather than cementing end to end. The same type 491 cement was used to make the mid-rib joints. The lattice consisted of six triangular cells arranged in a hexagonal pattern.

Temperature control was achieved using a Fisher model 126 muffle furnace. The lattice was placed in the furnace behind a calibrated length scale. Digital photographs were taken from the same height and angle for all measurements. Isolation from ambient temperature was achieved by taping a transparent plastic film over the furnace. A thermocouple lead was placed in the middle of the lattice for temperature measurements. Output indicated that the plastic film was a sufficient insulator from ambient temperature outside the furnace. With this configuration, digital photographs of the lattice in room temperature air were taken (25°C), followed by photographs at temperatures up to 120°C. Specifically the lattice was photographed in the furnace at ambient temperature, then the temperature was progressively increased. Further digital photographs of the lattice were taken at elevated temperature, then more photographs were taken during slow cooling. Some further experiments were conducted below ambient temperature by using the uniform low temperature outdoors in winter. Dimensions of the lattice in the vertical and horizontal directions were measured from the digital images using Photoshop software. The scale in the digital images was about 150 pixels/cm.

3 Analysis

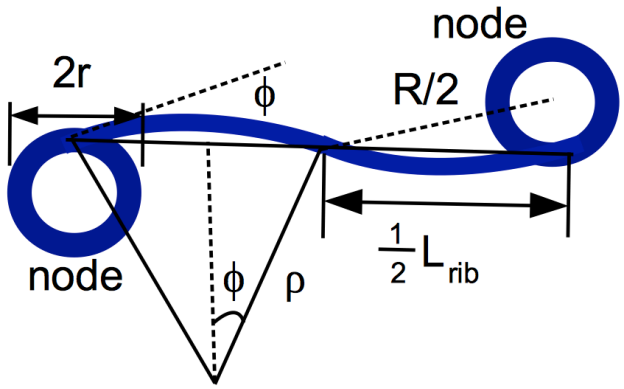

Figure 2: Bending of a rib in a chiral lattice structure.

Ribs are assumed to be sufficiently slender that deformation from axial strain is negligible in comparison with deformation due to bending of the ribs. Nodes are assumed to be rigid. Also, thermal expansion is assumed to occur freely without constraint. In the chiral lattice, strain is geometrically linked to rotation ϕ, node outer radius r and the spacing R of nodes between centers [7]:

$$\epsilon = \frac{r\phi}{R} \tag{1}$$

A temperature change causes bending of the bi-material rib segments which produces curvature with radius ρ in which the included angle is 2ϕ as shown in Figure 2. So

$$\phi = \frac{L_{rib}}{4\rho} \tag{2}$$

where the rib length L_{rib} is such that, from the diagram,

$$R = \sqrt{L_{rib}^2 + (2r)^2} \tag{3}$$

Each half of the rib has a uniform curvature but in the opposite direction because the bi-material strips have opposite orientation. Hence, the deformed rib has an S shape. Combining Eq. 1 - Eq. 3 yields

$$\epsilon = \frac{r}{4\rho} \frac{1}{\sqrt{1 + (2r/L_{rib})^2}} \tag{4}$$

The thermal expansion α is expressed in terms of specific curvature ${\rho_s}^{-1} = \rho^{-1}/\delta T$ so

$$\alpha = \frac{r}{4\rho_s} \frac{1}{\sqrt{1 + (2r/L_{rib})^2}}. \tag{5}$$

But the curvature is provided by the manufacturer [18] as a specific curvature parameter κ = 37 - 41 $\times 10^{-6} \frac{mm}{mm}{}^{\circ}\mathrm{C}^{-1}$ that incorporates the change of curvature with temperature change; in the following a value of 40 is used. ${\rho_s}^{-1} = \frac{\kappa}{h}$, so with h = 0.25 mm, substituting the dimensions and specification of κ in Eq. 5, the lattice has expansion of magnitude $\alpha = 320 \times 10^{-6}$ K^{-1}. The analysis does not provide the sign because orientation was not considered.

If one is provided with the elastic modulus and thermal expansion of each constituent, E_1 and α_1 for phase 1 and E_2 and α_2 for phase 2 respectively, and with the corresponding thickness a_1 and a_2 of each layer in the bi-material strip, then the curvature is [4],

$$\rho^{-1} = \frac{(\alpha_2 - \alpha_1)\delta T}{\frac{h}{2} + \frac{2(E_1 I_1 + E_2 I_2)}{h}[\frac{1}{E_1 a_1} + \frac{1}{E_2 a_2}]} \tag{6}$$

in which δT is temperature change, and $I_1 = \frac{a_1^3}{12}$ and $I_2 = \frac{a_2^3}{12}$ are the section moments of inertia of the layers. The total thickness is $h = a_1 + a_2$.

This lattice structure allows one to design the thermal expansion. Larger nodes give rise to a larger magnitude of thermal expansion. The sign of the expansion depends on the orientation of the bimetallic rib elements. Also, the specific curvature, hence the thermal expansion, will increase as the ribs become more slender (smaller h).

4 Results and discussion

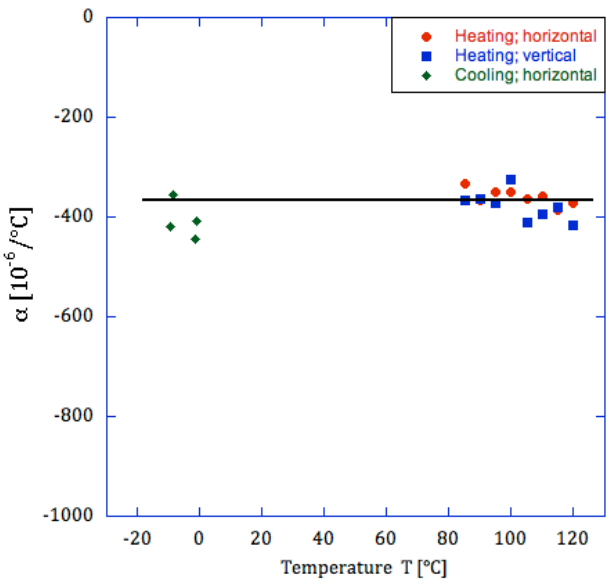

Figure 3: Experimentally determined thermal expansion coefficient α of the lattice vs. temperature. The lattice has no thermal strain at the reference temperature of 25°C

Experimentally determined thermal expansion vs. temperature is shown in Figure 3. The thermal expansion is negative, there is no systematic difference between expansion in the vertical and horizontal directions, and there is no systematic difference between heating and cooling. Measurements at small temperature deviations were limited by image resolution and are not shown. The straight line is a guide for the eye. Negative thermal expansion is uncommon in homogeneous materials; it entails contraction with increasing temperature and expansion with decreasing temperature. The lattice underwent substantial deformation at elevated temperature, sufficient to observe rib curvature, as shown in Figure 4. The maximum global strain, however, did not exceed 0.05.

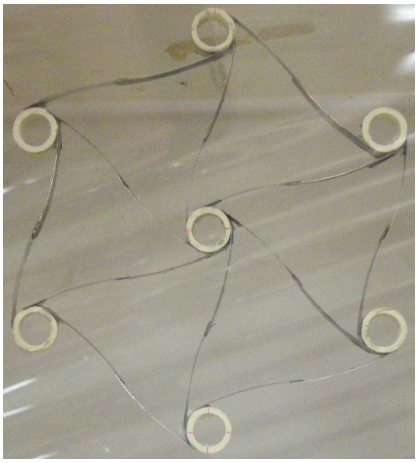

Figure 4: Deformation of lattice at 115°C in which ribs were initially straight at ambient temperature of 25°C. Horizontal and vertical refer to directions in which lattice expansion was measured.

The determination of thermal expansion α obtained via analysis and experiment are in reasonable agreement, in view of limits associated with resolution and the range of quoted specific curvature values. Also, the overlap of rib segments was not incorporated in the analysis. Too, the expansion of the polymer nodes is on the order 10^{-4} K^{-1} but the node diameter is only 1/5 the rib length. This contributes a reduction of about 5% in the total negative expansion of the lattice. The magnitude of α for the lattice is more than 30 times larger in magnitude than the α value for iron. Higher values could be obtained by using larger nodes, more slender ribs, or both. Positive thermal expansion can be achieved by reversing the orientation of the constituents of the rib elements.

Expansion can be made small by reducing the node radius r. Zero expansion is possible if the positive axial expansion of each rib element (not considered in the present analysis due to its relative smallness) is balanced by negative expansion due to rib bending. If the ribs have layers of equal thickness, their axial expansion could be balanced by contraction due to rib bending if $r < 0.5$ mm. This is comparable to the rib thickness and the thermal expansion is likely to be sensitive to variations in dimensions. So design for zero expansion by this approach would require high precision in the geometrical parameters. Zero expansion is also possible in other lattices [3] [20].

Node rotation for a single node was $\phi = 0.15$ rad for a temperature change of 33°C. Node rotation is consistent with the notion of homogenizing the lattice as a continuum via Cosserat elasticity. Cosserat solids incorporate rotational degrees of freedom in the microstructure in addition to the usual translation. There are additional elastic constants associated with sensitivity to gradients of rotation; in three dimensions there are six elastic constants for an isotropic, non-chiral Cosserat solid; nine constants if it is chiral. Cosserat solids exhibit an internal length scale in contrast to classically elastic solids; characteristic lengths are expressed in terms of ratios of tensorial elastic constants. Cosserat elastic constants were obtained via analysis of chiral lattices [10]. Cosserat elastic constants have been determined experimentally in several non-chiral foam materials from size effect experiments [21] [22]. Specifically, slender rods in torsion or bending are observed to be more rigid than anticipated based on classical elasticity. In these foams, the characteristic length is comparable to the cell size; for these materials, 0.3-3 mm. Rotations have been studied in the context of rotational waves [23] in designed granular materials. In Cosserat solids, concentrations of stress around holes and cracks is ameliorated, so there is a link to the toughness of the material. A continuum view is more appropriate to thermoelastic lattices such as the present ones than for piezoelectric lattices. Temperature changes can be imposed globally as with a homogeneous material; by contrast piezoelectric lattices thus far entail an electrical connectivity between layers that must be provided for the piezoelectric effect to be manifest. Local rotations in isotropic Cosserat elastic materials are driven by gradients in deformation. If the material is chiral, a uniform stretch gives rise, in three dimensions, to a twisting deformation, hence rotations [24]. Stretch-twist coupling of this kind has been analyzed for cholesteric elastomers [25]. In thermoelastic chiral materials or lattices such as the present lattice, a uniform temperature change gives rise to local rotations.

The sign of the thermal expansion and the sign of Poisson's ratio are independent. For example, the present lattice with Poisson's ratio -1 can be made with positive thermal expansion by reversing the rib orientation or by using homogeneous ribs. As for the freedom associated with Cosserat elasticity, the characteristic length can be made large or small by choice of the size of the cells in the lattice; small cells are possible via 3-D printing methods.

As for chiral lattices, such structures have been envisaged for chiral honeycomb [14] in sandwich panels for airplane wings that change shape. Chiral honeycombs of various type have also been optimized for buckling strength [26]. Related structures containing rotating hexamers and trimers [27] and stochastic distributions of circular node sizes can have negative Poisson's ratio of large

magnitude. Such structures do not have tunable thermal expansion but variants may be envisaged with such a capability. Indeed, bi-material elements in anti-tetrachiral honeycombs [28] have been analyzed via finite elements; negative properties can be obtained. In view of the additional freedom associated with thermal expansion, the present lattices may be considered further in this context or other lattices developed. The large thermal expansion of the lattice in comparison to its constituent metals can be useful in devices where a large response is desired from a small temperature change.

5 Conclusion

The effective thermal expansion coefficient of the chiral lattice is about $\alpha = -3.5 \times 10^{-4} \mathrm{K}^{-1}$. This is much larger in absolute magnitude than the value for known homogeneous materials. The thermal expansion can be controlled by varying the geometrical parameters of the lattice.

Acknowledgment

Partial support from the NSF via CMMI-1361832 and from DARPA-LLNL under the aegis of Dr. Judah Goldwasser is gratefully acknowledged.

References

[1] J. L. Cribb, Shrinkage and thermal expansion of a two-phase material, Nature, **220**, 576-577 (1963).

[2] R. S. Lakes, Cellular solid structures with unbounded thermal expansion, J. of Materials Science Letters, **15**, 475-477 (1996).

[3] R. S. Lakes, Solids with tunable positive or negative thermal expansion of unbounded magnitude, Applied Phys. Lett. **90**, 221905 (2007).

[4] S. P. Timoshenko, Analysis of bi-metal thermostats, J. Optical Soc. America, **11**, 233-355 (1925).

[5] R. S. Lakes, Piezoelectric composite lattices with high sensitivity, Philosophical Magazine Letters **94**, (1), 37-44 (2014).

[6] B. Rodriguez, H. Kalathur, and R. S. Lakes, A sensitive piezoelectric composite lattice: experiment, Phys. Stat. Sol. (b) **251**(2) 349-353 (2014).

[7] D. Prall and R. S. Lakes, Properties of a chiral honeycomb with a Poisson's ratio -1, Int. J. of Mechanical Sciences, **39**, 305-314, (1996).

[8] R. S. Lakes, Foam structures with a negative Poisson's ratio, Science, **235** 1038-1040 (1987).

[9] L. J. Gibson, M. F. Ashby, G. S. Schajer, and C. I. Robertson, The mechanics of two dimensional cellular solids, Proc. Royal Society London, **A382**, 25-42 (1982).

[10] X. N. Liu, G. L. Huang, G. K. Hu, Chiral effect in plane isotropic micropolar elasticity and its application to chiral lattices, J. of the Mechanics and Physics of Solids **60**, 1907-1921 (2012).

[11] A.C. Eringen, Theory of micropolar elasticity. In Fracture Vol. **1**, 621-729 (edited by H. Liebowitz), Academic Press (1968).

[12] A. Spadoni, M. Ruzzene, Elasto-static micropolar behavior of a chiral auxetic lattice, J. of the Mechanics and Physics of Solids **60**, 156-171 (2012).

[13] D. Bornengo, F. Scarpa, C. Remillat, Evaluation of hexagonal chiral structure for morphing airfoil concept, Proceedings of the Institution of Mechanical Engineers, Part G: Journal of Aerospace Engineering **219** 185-192 (2005).

[14] J. Martin, J. Heyder-Bruckner, C. Remillat, F. Scarpa, K. Potter, M. Ruzzene, The hexachiral prismatic wingbox concept, Phys. Stat. Sol. (b) **245** 570-571 (2008).

[15] A. Spadoni, M. Ruzzene and F. Scarpa, Global and local linear buckling behavior of a chiral cellular structure, Phys. Stat. Sol. (b) **242** 695-709 (2005).

[16] A. Spadoni, M. Ruzzene, S. Gonelli, F. Scarpa, Phononic properties of hexagonal chiral lattices, Wave Motion **46** (7), 435-450 (2009).

[17] H. Abramovitch, M. Burgard, L. Edery-Azulay, K.E. Evans, M. Hoffmeister, W. Miller, F. Scarpa, C.W. Smith, K.F. Tee, Smart tetrachiral and hexachiral honeycomb: Sensing and impact detection, Composites Science and Technology **70**, 1072?1079 (2010).

[18] Engineered materials solutions specification sheet, Engineered Materials Solutions, 39 Perry Avenue, Attleboro, MA 02703

[19] U. S. patent US 2982646

[20] J. J. Lehman, and R. S. Lakes, Stiff, strong zero thermal expansion lattices via the Poisson effect, Journal of Materials Research, 29, 2499-2508, (2013).

[21] R. S. Lakes, Experimental microelasticity of two porous solids, Int. J. Solids and Structures, **22** 55-63 (1986).

[22] W. B. Anderson and R. S. Lakes, Size effects due to Cosserat elasticity and surface damage in closed-cell polymethacrylimide foam, Journal of Materials Science, **29**, 6413-6419, (1994).

[23] A. Merkel, V. Tournat, and V. Gusev, Experimental evidence of rotational elastic waves in granular phononic crystals, Phys. Rev. Lett. **107**, 225502 (2011).

[24] R. S. Lakes and R. L. Benedict, Noncentrosymmetry in micropolar elasticity, International Journal of Engineering Science, **29** (10), 1161-1167, (1982).

[25] M. Warner, E. M. Terentjev, R. B. Meyer, and Y. Mao, Untwisting of a cholesteric elastomer by a mechanical field, Phys. Rev. Lett. **85**, 2320-2324, (2000).

[26] W. Miller, C.W. Smith, F. Scarpa, K.E. Evans, Flatwise buckling optimization of hexachiral and tetrachiral honeycombs, Composites Science and Technology, **70**, 1049-1056, (2010).

[27] A. A. Pozniak and K. W. Wojciechowski, Poisson's ratio of rectangular anti-chiral structures with size dispersion of circular nodes, Phys. Stat. Sol. (b) **251**, 367-374, (2014).

[28] R. Gatt and J. N. Grima, Negative Compressibility, Physica Status Solidi Rapid Research Letters, **2**, 236-238, (2008).